

## Physicochemical and functional characteristics of lentil starch

M. Joshi<sup>a</sup>, P. Aldred<sup>a</sup>, S. McKnight<sup>b</sup>, J.F. Panozzo<sup>c</sup>, S. Kasapis<sup>d</sup>, R. Adhikari<sup>e</sup>, B. Adhikari<sup>a,\*</sup>

<sup>a</sup> School of Health Sciences, University of Ballarat, Mount Helen, VIC 3353, Australia

<sup>b</sup> School of Science, Information Technology and Engineering, University of Ballarat, Mount Helen, VIC 3353, Australia

<sup>c</sup> Department of Primary Industries, Horsham, VIC 3401, Australia

<sup>d</sup> School of Applied Sciences, RMIT University, Melbourne, VIC 3001, Australia

<sup>e</sup> CSIRO Materials Science and Engineering, Clayton South, VIC 3169, Australia

### ARTICLE INFO

#### Article history:

Received 9 July 2012

Received in revised form 11 October 2012

Accepted 12 October 2012

Available online 23 October 2012

#### Keywords:

Lentil starch

Amylose-to-amylopectin ratio

Rheological properties

Texture profile analysis

Stress relaxation

IR spectra

### ABSTRACT

The physicochemical properties of lentil starch were measured and linked up with its functional properties and compared with those of corn and potato starches. The amylose content of lentil starch was the highest among these starches. The crystallinity and gelatinization enthalpy of lentil starch were the lowest among these starches. The high amylose: amylopectin ratio in lentil starch resulted into low crystallinity and gelatinization enthalpy. Gelatinization and pasting temperatures of lentil starch were in between those of corn and potato starches. Lentil starch gels showed the highest storage modulus, gel strength and pasting viscosity than corn and potato starch gels. Peleg's model was able to predict the stress relaxation data of these starches well ( $R^2 > 0.98$ ). The elastic modulus of lentil starch gel was less frequency dependent and higher in magnitude at high temperature (60 °C) than at lower temperature (10 °C). Lentil starch is suitable where higher gel strengthened pasting viscosity are desired.

© 2012 Elsevier Ltd. All rights reserved.

### 1. Introduction

Lentil (*Lens culinaris*, M.) is one of the most important crops belonging to leguminosae family. Lentil seeds contain about 69% carbohydrates and most of which is present in the form of starch (Adsule & Kadam, 1989; Jood, Bishnoi, & Sharma, 1998). The starch in lentils is mainly distributed in the cotyledons dispersed in protein matrix and exists in granular form. According to FAO Statistics (2010) total world production of lentil was 4.58 million metric tonnes. Lentils are shipped after primary processing, therefore, there is a great deal of opportunity to develop value added products. Hence, greater understanding of physicochemical characteristics of lentil starch, which is the major constituent, is essential in providing sound scientific basis for new product development.

Starches are ubiquitous macromolecules synthesized by plants and have wide application in both food and non-food products (Lillford & Morrison, 1997). In food, starch is used as the major ingredient as well as a minor ingredient imparting some specific functions (Jane, 1997). Some of these functions include thickening, coating, gelling, adhesion, and encapsulation. When starch is heated in the excess of water, at a characteristic temperature range it swells irreversibly and undergoes order-to-disorder phase

transition (Cook & Gidley, 1992). This phenomenon is known as gelatinization and the characteristic temperature range at which this transition occurs is called gelatinization temperature. Gelatinization temperature is unique and characteristic to the starch source. Important functional properties of starch such as pasting and gelation are derived once the starch is gelatinized. The gelatinization results into swelling of starch granules, loss of crystallinity, uncoiling and dissociation of double helices (crystal melting) and finally disruption of the starch granules (Biliaderis, Grant, & Vose, 1979; Donovan, 1979; Parker & Ring, 2001). At high concentration, starch forms a three dimensional gel network, retards phase separation and provides basic structure to food products such as bread, cakes and puddings.

Starch is comprised of amylose and amylopectin, however, the size, shape and the composition (amylose to amylopectin ratio) of starch vary with botanical origin. Differences in starch physicochemical characteristics have significant impact on their functional properties, affecting their suitability for specific and targeted use. Based on the requirement of food products, starch from different sources possessing different physicochemical characteristics have to be selected to meet the specific processing needs. For example, high amylose starch is preferred for fried food coating batter due to its film forming properties that provides crispy texture in deep fried products (Jane, 1997). High amylose starch is also known to have excellent film forming properties (Fu, Wang, Li, Wei, & Adhikari, 2011). Amylose content of lentil starch is high and ranges from 29 to 45.5% (Hoover & Sosulski, 1991).

\* Corresponding author. Tel.: +61 3 53279249; fax: +61 3 5327 9840.

E-mail address: [b.adhikari@ballarat.edu.au](mailto:b.adhikari@ballarat.edu.au) (B. Adhikari).

Starch granules are semi-crystalline in nature consisting of ordered and disordered regions. The double helices formed by short amylopectin chains are involved in the formation of the crystallites in starch granules while disordered or amorphous regions are believed to be made up of amylose (Bogacheva, Wang, Wang, & Hedley, 2002). The amylose-to-amylopectin ratio has great impact on the structure–function property of starch (Tester, 1997).

Pasting and gel formation are the two most important functional properties of starch. The understanding of these functional characteristics is essential in food processing operations involving starch. The understanding of the rheological properties helps in the selection of ingredients to suit the end product requirements. Corn and potato starches have been extensively investigated, readily available and commonly used in food processing (Silverio, Fredriksson, Andersson, Eliasson, & Aman, 2000). Similar studies on lentil starch are very limited and there is a lack of information on the structure–function relationship of this starch.

The limited publications on lentil starch mainly deal with chemical composition, granule morphology, molecular weight, crystallinity and gelatinization properties (Biliaderis et al., 1979; Bhatti & Slinkard, 1979; Hoover & Ratnayake, 2002). Most of the functional properties covered in these publications are based on RVA or Barbender methods (Hoover & Manuel, 1995; Kaur, Sandhu, & Lim, 2010). Study on small amplitude oscillation rheological properties in lentil starch are quite limited (Ahmed & Auras, 2011). Some publications also reported the chemical and physical modification of lentil starches (Chung, Liu, & Hoover, 2009; Hoover & Manuel, 1995; Hoover & Sosulski, 1986) to increase resistance towards mechanical shearing, acid hydrolysis, high temperatures and/or enzyme hydrolysis. These works mostly deal with the correlation of physicochemical properties with in vitro digestibility of starch. The use of chemically modified starch is not popular with consumers and is restricted by legislation (Lillford & Morrison, 1997). There is a lack of systematic study linking the physicochemical properties with functional and rheological properties of lentil starch. Thus the purpose of this work was to measure the physicochemical properties of lentil starch (composition, crystallinity, gelatinization behaviour) and relate these measurements with functional properties such as swelling, pasting and gelation. Relatively well studied starches such as corn and potato starch are used for comparison.

## 2. Materials and methods

### 2.1. Raw materials

The lentil starch was isolated from Aldinga cultivar of lentil (Section 2.2). The lentil seeds were provided by Department of Primary Industries, Horsham, Australia. Corn starch and potato starch were purchased from Ajax Chemicals, NSW, Australia.

### 2.2. Isolation and purification of starch

Starch was isolated by wet method. Dehulled lentils were pulverized into lentil flour using a disc mill with 0.5 mm aperture. Lentil flour was suspended in water (1:10, w/v) and pH of the suspension was adjusted to 8.0 with 1 M NaOH/HCl and mixed using a magnetic stirrer at ambient condition ( $20 \pm 2^\circ\text{C}$ ) to solubilize the protein and thus facilitate the separation of starch. The mixture was allowed to settle for 2–3 h and supernatant was removed by centrifuging at 17,500 g in a centrifuge (Sorvall SS34) for 15 min. The starch was washed by resuspending in distilled water for 3–4 times and the supernatant was decanted off. Finally, starch dispersion was sieved through series of US standard sieve sizes of 120, 170 and 325. Purified starch was then dried in a custom-built air

dryer (Adhikari, Howes, Shrestha, Tsai, & Bhandari, 2006) at  $35^\circ\text{C}$  for 24 h and the dried starch sample was kept in a sealed container at  $4^\circ\text{C}$  until further use.

### 2.3. Physicochemical properties of starch

#### 2.3.1. Proximate composition

Starch samples were analysed for their moisture (Method No. 925.1), crude protein ( $\text{N} \times 6.25$ ) (Method No. 920.87) and ash content (Method No. 923.03) following the standard method of analysis (AOAC, 2005).

#### 2.3.2. Amylose content

Amylose content of the isolated lentil starch along with the corn and potato starch was determined by using amylose/amylopectin kit from Megazyme (Wicklow, Ireland). This method uses the specific binding of Concanavalin A to non-reducing end groups of amylopectin and thus precipitates this fraction of the starch.

#### 2.3.3. Starch morphology

Starch morphology of the lentil starch along with the corn and potato starch was studied by scanning electron microscope (SEM) (JEOL, JSM 6300 SEM, Japan). For SEM, very thin layer of starch powder was directly applied to double-sided adhesive tape on an aluminium stub and was coated with gold. An accelerating potential of 15 kV was used during micrography during image acquisition.

#### 2.3.4. Light microscopy

Birefringence of native and heated (lentil, corn and potato) starch suspensions were observed under polarized and non-polarized light with a microscope fitted with a digital camera (Canon EOS 60D, Canon Ltd.). The images were recorded at  $100\times$  magnification for all starch samples.

#### 2.3.5. Fourier transform infrared spectroscopy (FTIR)

Infrared spectra of dry starch powder and starch suspension in water and thermally treated starch suspensions ( $90^\circ\text{C}$ , 10 min) were recorded on a Nicolet 6700-FTIR (ThermoScientific, Waltham, MA, USA) equipped with a thermoelectrically cooled deuterated triglycine sulphate (DTGS). The iTR attenuated total reflectance (ATR) sampling accessory was used in these tests. Each specimen was applied on to the face of diamond crystals of the sample accessory. IR spectra were collected in the range of  $4000\text{--}625\text{ cm}^{-1}$  at a resolution of  $4\text{ cm}^{-1}$ . For each sample, 50 scans were carried out and averaged. Raw spectra were baseline corrected and deconvoluted by using Omnic software (Thermo Scientific).

#### 2.3.6. X-ray diffraction (XRD)

X-ray diffraction (XRD) traces of the lentil starch granules were measured using a Siemens (D501, Siemens, Karlsruhe, Germany) diffractometer with  $\text{CuK}\alpha < 1$  radiation. Diffractograms were recorded between  $5^\circ$  and  $35^\circ$  ( $2\theta$ ) at a rate of  $1.20^\circ/\text{min}$  ( $2\theta$ ) and with a step size of  $0.05^\circ$  ( $2\theta$ ). Crystallinity of the starch was determined following the method of Nara and Komiya (1983). With this method, crystallinity is calculated by dividing the area under the crystalline peaks by the total area under the diffractogram. Background fitting and areas were measured by using Traces (version 6.0) software program.

#### 2.3.7. Granule particle size

The particle size distribution of the starch samples was measured using a Malvern laser diffraction particle size analyser (Mastersizer 2000<sup>TM</sup>, Malvern Instrument, USA). Water was used as a dispersing medium for all the powders. The refractive index values used for water and starch were 1.33 and 1.41 respectively. The

sample suspension was subjected to sonication during measurements for better dispersion of the powder. Particle size distribution was calculated by the Mastersizer software (version 5.54) and expressed as 10, 50 and 90% volume based size ( $D_{v,10}$ ,  $D_{v,50}$ ,  $D_{v,90}$ ).

### 2.3.8. Gelatinization properties

Gelatinization properties (onset and peak gelatinization temperatures, enthalpy of gelatinization) of starch samples were studied by using a differential scanning calorimeter (DSC) in which starch samples in excess of water were heated in hermetically sealed pans (Mettler Toledo, Switzerland). Starch sample ( $3.5 \pm 0.5$  mg, dry wet basis, dwb) was weighed into standard aluminium pan of 40  $\mu$ l capacity into which 10  $\mu$ l of distilled water was added with micropipette. Samples were hermetically sealed and allowed to stand for at least 1 h before heating in DSC. The DSC was calibrated using indium (melting enthalpy and peak melting point of 27.93 J/g and 157.93 °C, respectively). Sample pans along with empty pan as reference was heated at a rate of 10 °C/min from 25 °C to 100 °C. Onset temperature ( $T_o$ ), peak temperature ( $T_p$ ) and enthalpy of gelatinization ( $\Delta H$ ) were calculated using STAR<sup>®</sup> software associated with the DSC.

### 2.3.9. Swelling power

Swelling power of starch samples was determined at different temperatures (60–90 °C) by using method of [Leach, McCowen, and Schoch \(1959\)](#). Starch swelling power was calculated as the ratio of weight of swollen starch to the initial dry weight of the starch and expressed as g/g. The temperature dependency of swelling power of starch granule was predicted by using following models:

#### (a) Vogel–Tamman–Fulcher (VTF)

$$x = x_o + Ae^{-(B/T) - T_{ref}} \quad (1)$$

#### (b) Power law

$$x = x_o + K_{sw}(T - T_{ref})^n \quad (2)$$

where  $x_o$  and  $x$  are the weight of the starch at  $T_{ref}$  and  $T$  temperature respectively. The reference temperature ( $T_{ref}$ ) used for this calculation was 60 °C.  $A$  and  $B$  are the constants for VTF equation and  $K_{sw}$  is the constant for power law equation.

### 2.3.10. Pasting properties

Pasting profiles and viscosity profiles of starch samples were measured by using Rapid ViscoAnalyzer (Newport, Scientific Pty Ltd., NSW, Australia). The Rapid Visco-Analysis (RVA) is a common viscometric method to determine pasting properties of starch in which viscosity profile of starch suspension is recorded against time during heating and subsequent cooling. Viscosity of paste is expressed as mPa s. Starch concentration of 8% (w/w) was used in all these tests. The starch suspensions were heated from 50 °C to 95 °C at the heating rate of 12.5 °C/min, held at 95 °C for 5 min and finally cooled down to 50 °C at the same cooling rate. During heating, the samples were stirred at 960 rpm for the first 1 min and 160 rpm for the rest of testing time.

### 2.3.11. Rheological properties of starch gels

Rheological parameters (elastic ( $G'$ ) and viscous ( $G''$ ) moduli) of starch pastes and gels (15%, w/v) were measured using HAAKE Rheostress I (ThermoFisher, Germany) with plate and plate parallel geometry (PP 35Ti) with 35 mm diameter. Starch suspension was prepared by heating at 60 °C with continuous stirring at 300 rpm for 10 min using a magnetic stirrer.

**2.3.11.1. Temperature sweep.** Well mixed starch suspension at  $60 \pm 2$  °C was poured on the lower plate of the rheometer. The temperature of the plate was maintained at  $60 \pm 2$  °C as well before the sample was poured in. The sample was then heated from 60 °C to 90 °C at heating rate of 2 °C/min, held at 90 °C for 10 min and finally cooled down to 60 °C at the cooling rate of 0.6 °C/min. During temperature sweep, storage modulus ( $G'$ ), loss modulus ( $G''$ ) and loss tangent ( $\delta$ ) of the gels were recorded at constant frequency of 1 Hz and shear stress of 1 Pa as a function of time.

**2.3.11.2. Frequency sweep.** Dynamic frequency sweep tests were performed on gels which were formed in situ during the temperature sweep tests. The frequency dependence of the elastic ( $G'$ ) and viscous ( $G''$ ) moduli was recorded within the linear viscoelastic regime. Frequency sweep was run from 0.001 to 10 Hz at a shear stress of 10 Pa at two temperatures (60 and 10 °C) to investigate the effect of temperature on the gel behaviour. The degree of frequency dependence expressed by the constant ' $n$ ' was calculated as proposed by [Egelandsdal, Fretheim, and Samejima \(1986\)](#)

$$G' = Kf^n \quad (3)$$

where  $G'$  is the storage modulus (Pa),  $f$  is the oscillation frequency (Hz) and  $K$  is a constant. The constant  $n$  is the slope for log-log plot of  $G'$  versus  $f$  curve.

### 2.3.12. Texture profile analysis (TPA) of starch gel

Texture profile analysis (TPA) of starch gels was carried out using a texture analyser (TA.XT plus, Stable Micro Systems Ltd., UK). The TPA tests were performed and data were analysed following [Bourne's method \(2002\)](#). The starch paste for texture analysis was prepared from starch suspension as mentioned above in Section 2.3.11 in a plastic tube and heated in a water bath at 90 °C with continuous mixing for 10 min followed by immediate cooling under tap water. The gel was stored overnight at 4 °C and equilibrated to room temperature (25 °C) for at least 30 min before performing measurement. Gel cylinders of 8.2 mm diameter and 8 mm height were cut with stainless-steel cutter. Each gel sample was compressed twice to 30% of their original height at a constant speed of 0.3 mm/s with 5 s time gap was used in between two compression cycles. A cylindrical probe (derlin) of 10 mm diameter was used for this purpose. Texture profile analysis (TPA) was carried out on force–time curves to calculate hardness, cohesiveness, adhesiveness, springiness, and gumminess.

### 2.3.13. Stress relaxation properties

A stress relaxation test of the starch gels was conducted using the texture analyser to determine their viscoelastic properties. The preparation of gel and the test conditions used were similar to those used in TPA test. When a viscoelastic material is compressed and allowed to relax, the stress decays. In this experiment, a gel is deformed to a fixed strain and the strain is held constant and the stress is allowed to vary as required to maintain the given strain. The test was performed using a cross-head speed of 0.3 mm/s. The gel specimens were compressed to 30% deformation and allowed to relax for 600 s. Triplicate tests were performed for all the samples. The force–time data were recorded using Exponent<sup>TM</sup> software associated with the texture analyser. The force was normalized to express as stress ( $\sigma_t$ ) in Pa by using the cross-section area of the un-perturbed gel (Eq. (4)).

$$\sigma_t = \frac{F_t}{A} \quad (4)$$

where  $F_t$  (N) is the force measured over time (s) and  $A$  (m<sup>2</sup>) is the cross-section area of the un-perturbed gel.

The stress-relaxation parameters were determined in experiments of short period by using a mathematical model suggested

**Table 1**  
Physicochemical properties of lentil, corn and potato starch.

Parameters		Lentil starch	Corn starch	Potato starch
Protein (g/100 g)		0.36 ± 0.03 <sup>a</sup>	0.43 ± 0.03 <sup>b</sup>	0.27 ± 0.02 <sup>c</sup>
Ash (g/100 g)		0.17 ± 0.05 <sup>a</sup>	0.21 ± 0.03 <sup>a</sup>	0.36 ± 0.04 <sup>b</sup>
Amylose (%)		32.52 ± 3.52 <sup>a</sup>	24.78 ± 2.52 <sup>b</sup>	14.93 ± 0.83 <sup>c</sup>
Relative crystallinity (%)		9.12 <sup>a</sup>	25.37 <sup>b</sup>	37.67 <sup>c</sup>
Starch granule size (μm)	D <sub>v</sub> (0.1)	14.43 ± 0.02 <sup>a</sup>	7.50 ± 0.14 <sup>b</sup>	22.83 ± 0.02 <sup>c</sup>
	D <sub>v</sub> (0.5)	21.57 ± 0.03 <sup>a</sup>	12.93 ± 0.02 <sup>b</sup>	44.15 ± 0.03 <sup>c</sup>
	D <sub>v</sub> (0.9)	32.21 ± 0.05 <sup>a</sup>	20.03 ± 0.64 <sup>b</sup>	76.06 ± 0.06 <sup>c</sup>
	Onset temperature (°C)	61.56 ± 0.23 <sup>a</sup>	68.58 ± 0.49 <sup>b</sup>	60.43 ± 0.23 <sup>c</sup>
	Peak temperature (°C)	69.32 ± 0.30 <sup>a</sup>	73.8 ± 0.25 <sup>b</sup>	65.65 ± 0.23 <sup>c</sup>
Gelatinization properties	Heat enthalpy (J/g)	11.80 ± 1.04 <sup>a</sup>	14.80 ± 0.67 <sup>b</sup>	18.28 ± 0.23 <sup>c</sup>

All the data are the mean of three replicates and are expressed as mean ± SD.

Means with the different superscript letters within the same row are significantly different ( $p < 0.05$ ).

by Peleg (1980) Eq. (4) to characterize the relaxation behaviour of starch gels.

$$\sigma_t = \sigma_0 - \frac{\sigma_0 t}{k_1 + k_2 t} \quad (5)$$

where  $\sigma_0$  is the initial stress (Pa) at  $t \rightarrow 0$ , applied for compression,  $\sigma_t$  is the decaying stress as a function of time,  $k_1$  and  $k_2$  are constants. These constants are independent of the relaxation time. The reciprocal of  $k_1$  represents the initial decay rate. Constant  $k_1$  represents the amount of stress that remains unrelaxed. If  $k_1 = 0$ , all the stress relaxes and the material is considered to be a purely viscous liquid. If  $k_1 > 0$ , there is a residual stress even when  $t \rightarrow \infty$  and the material is viscoelastic solid or liquid. A decrease in initial decay rate indicates an increase in resistance to elastic deformation. The magnitude of  $k_1$  can be used to measure the solidity (for viscoelastic liquid the stress relaxed to zero, while for a viscoelastic solid it asymptotically approaches an equilibrium stress). Constant  $k_2$  represents the rate at which stress relaxes. An increase in the value of  $k_2$  means the elastic component present in the sample is increasing (Jaya & Durance, 2008). For an ideal elastic solid,  $k_2 = 0$  (Peleg, 1980). The equilibrium relaxation stress,  $\sigma_\infty$  (Pa) at  $t \rightarrow \infty$  was estimated by using Eq. (5).

$$\sigma_\infty = \sigma_0 - \frac{\sigma_0}{k_2} \quad (6)$$

#### 2.4. Statistical analysis

Triplicate runs were carried out for each experiment, if not stated otherwise. Data were subjected to statistical analysis, using one way analysis of variance (ANOVA) to evaluate the significance of differences ( $p < 0.05$ ). SPSS version 10.0 software (SPSS Co., Chicago, U.S.) was used for this purpose.

### 3. Results and discussion

#### 3.1. Physicochemical properties

##### 3.1.1. Chemical composition of starch

Chemical composition of all three starch samples is presented in Table 1. Ash and crude protein content of three starches ranged from 0.27 to 0.43 g/100 g and 0.17 to 0.36 g/100 g, respectively. Ash content in corn and potato starch was slightly higher than lentil starch. Low ash and protein content in starch indicates the purity of starch. According to Tester, Karkalas, and Qi (2004), purified starches should contain less than 0.6% protein. Three starches were significantly different ( $p < 0.05$ ) in amylose content. The amylose content of lentil starch was 32.52% which is within the range of previously published data (Hoover & Sosulski, 1991). Legume starches are characterized by high amylose content. The amylose content of corn and potato starch was found to be 24.78% and 14.93%, respectively.

##### 3.1.2. Granule morphology of lentil starch granules

The scanning electron micrographs (SEM) and light microscopic images of lentil starch granules were large oval to small round as shown in shape Fig. 1 (panels a, b and c). The surface of the starch granule was smooth and did not show any fissures. Similar results were reported by other workers (Bhatti & Slinkard, 1979; Hoover & Manuel, 1995). The birefringence (Maltese-cross) pattern of lentil starch in native state is shown in Fig. 1 (panel d). Starch granules showed well defined maltase-cross when heated up to 60 °C (Fig. 1, panel e and f) and was completely disappeared after heating beyond 70 °C. Weaker birefringence patterns are indicative of disorganized amylopectin double helices within the crystalline lamella of starch granules (Ambigaipalan et al., 2011). The internal structure of starch granule is concentrically layered and the growth rings are clearly visible in large granules. However, such layers are not visible in small granules (Fig. 1, panel c). The growth rings are made up of repeating layers of crystallized terminal chains of amylopectin interlaid with amorphous regions of amylose and amylopectin molecules.

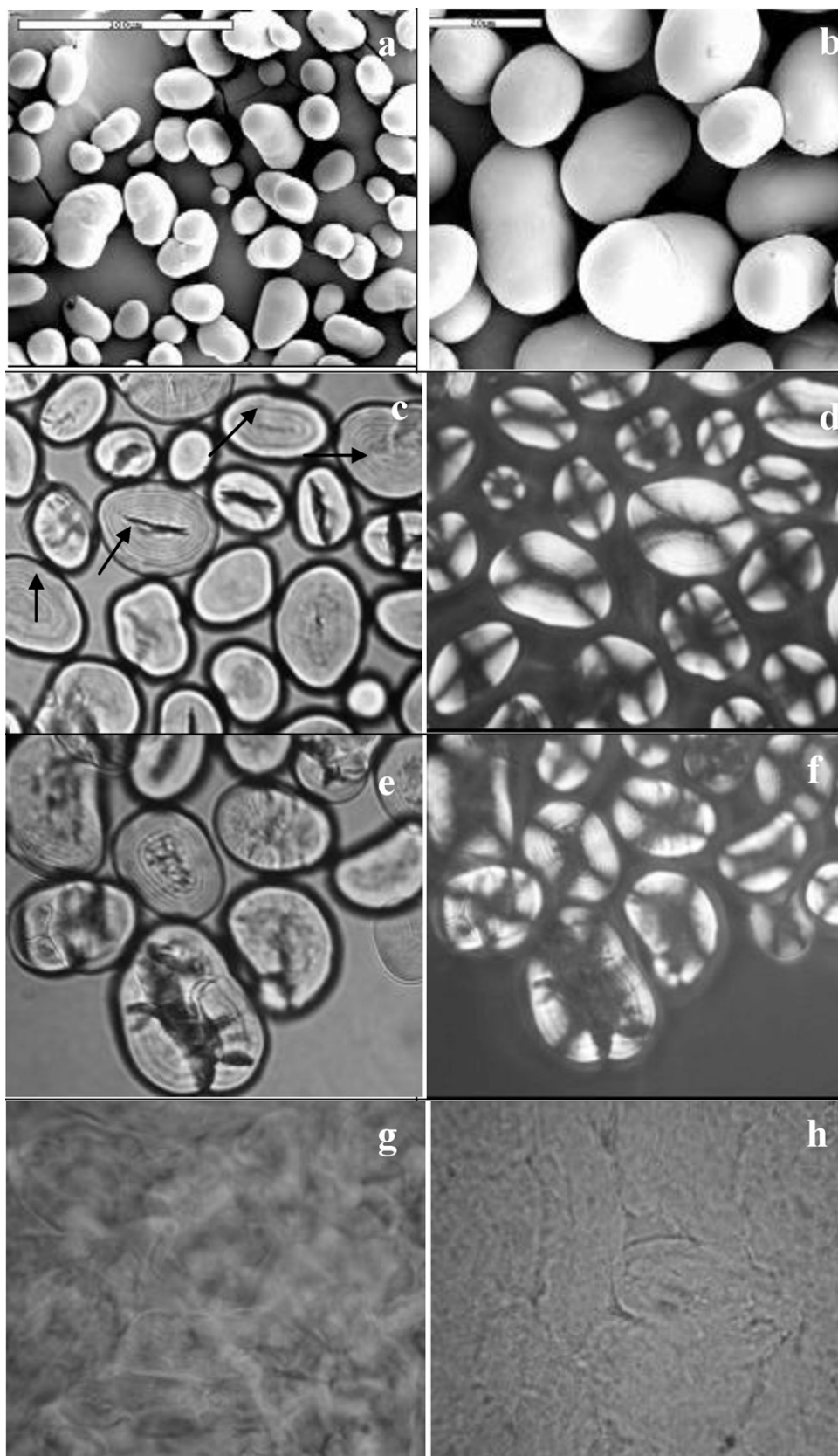
##### 3.1.3. Particle size distribution of starches

Fig. 2 illustrates the granule (particle) size distribution of lentil, corn and potato starches. The granule or particle size and shape of starch vary greatly with botanic origin. Larger granules tend to swell more on cooking and hence granule size is an important factor affecting the starch functionality. Among three starches, potato and corn exhibited bimodal particle size distribution with the size of small granule fractions ranging from 0.8 to 5 μm and 0.5 to 3 μm respectively. Lentil starch granules showed monomodal size distribution with narrow size range (10–45 μm) and the mean granule size was 21.57 μm ( $D_v$ , 0.5). The potato starch showed the highest mean granule size (44 μm) and the widest particle size distribution (Fig. 2) while the corn starch has the smallest granule size (12.93 μm) (Table 1). These particle size and size distribution data are within range of other published data (Hoover, Hughes, Chung, & Liu, 2010; Tester et al., 2004).

##### 3.1.4. Crystallinity of starches

The X-ray diffraction pattern of the lentil, corn and potato starch is shown in Fig. 3. Corn starch and potato starches exhibited characteristic A and B type crystalline patterns, respectively while lentil starch showed C type crystalline pattern. C type diffraction pattern is intermediate between A (cereals) and B (tubers) type diffraction patterns and is common in legume starches (Hoover & Ratnayake, 2002). Starch granules are semi-crystalline and consist of both amorphous and ordered (crystalline) areas. These ordered areas are formed from the short chains within amylopectin molecules being arranged in clusters. Short and long range order structures have been identified within the ordered areas. The short-range order structures have been found to consist of parallel-stranded double helices, and the long-range order arrangements of these double





**Fig. 1.** Photomicrographs of lentil starch: (a and b) SEM of lentil starch; (c) lentil starch without and (d) with polarized light (100×); (e) lentil starch suspension heated at 60 °C with and (f) without polarized light (100×); (g) lentil starch suspension heated to 85 °C when hot and (h) after cooling (100×).

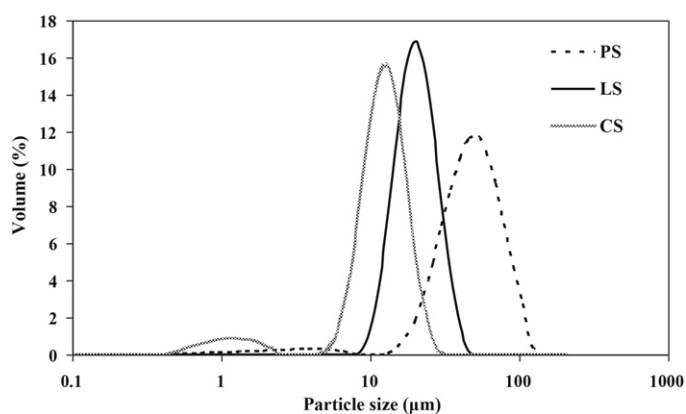


**Fig. 2.** Particle size distribution pattern of lentil starch (LS), corn starch (CS) and potato starch (PS).

helices give rise to two types of (A and B) crystalline or polymorphic structures (Bogracheva et al., 2002). Lentil starches exhibited five major peaks at  $5.6^\circ$ ,  $15.0^\circ$ ,  $17.0^\circ$ ,  $17.8^\circ$ ,  $23.0^\circ$  and  $26.3^\circ$  ( $2\theta$  angles), of which, three peaks at  $15^\circ$ ,  $17^\circ$  and  $26.3^\circ$  ( $2\theta$  angle) were common among three starches. Two peaks at  $17.8^\circ$  and  $23^\circ$  ( $2\theta$  angle) were common between lentil and corn starch. Likewise, the peak at  $5.6^\circ$  ( $2\theta$  angle), characteristics of B-type diffraction pattern was observed in both lentil and potato starch, however, the intensity of peaks for the latter was much higher than in the former. Higher peak values indicate the better orientation and/or more compactly packed crystallites within the granules, therefore, diffract X-rays to greater degree (Hoover & Manuel, 1995).

The degree of crystallinity is a valuable parameter to consider as it influences properties of the starch or starch containing products. Crystal types are inherent to the molecular properties of starch and are direct results of the amylose content and the average chain length in the corresponding amylopectin (Cheetham & Tao, 1998). The varying degree of crystallinity in these three starches is evidenced from the diffractogram shown in Fig. 3 which shows higher intensity in the major peaks for potato and corn starches compared to that of the lentil starch. The crystallinity of the three starches was in the following order: potato starch > corn starch > lentil starch and ranged from 9.12 to 37.67% (Table 1). The percentage of crystallinity in these three starch types agrees with the published data (Hoover et al., 2010; Tester et al., 2004). The crystallinity of starch is affected by the size of the crystals, amount of crystalline regions (influenced by the content and chain length of amylopectin), orientation of the double helices within the crystalline domains and the extent of interaction between double helices (Ambigaipalan et al., 2011). The higher crystallinity of potato starch reflects stronger interaction between double helices

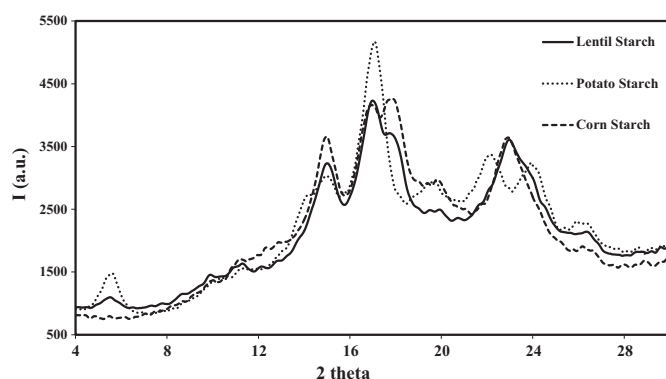


**Fig. 3.** X-ray diffractogram of lentil, corn and potato starches in native state.

**Table 2**

Major FTIR bands ( $\text{cm}^{-1}$ ) in lentil starch/lentil gel and their band assignment.

Bands ( $\text{cm}^{-1}$ )		Band assignment <sup>a</sup>
Lentil starch	Lentil starch gel	
3326.1	3326.1	O—H stretching (Kacurakova and Mathlouthi, 1996; van Soest et al., 1995)
2930	2932.9	CH <sub>2</sub> deformation (Kacurakova and Mathlouthi, 1996; Kizil et al., 2002)
2891	2887.5	
—	2752, 2632, 2522.9, 2488.4	
1641	—	Water adsorbed in the amorphous part of the starch (Kizil et al., 2002; Wilson et al., 1991)
1456.7	1456.7	1454.9: CH bending (Yao, Zhang, & Ding, 2002)
1416.3	—	CH <sub>2</sub> bending, COO— stretching (Kacurakova and Mathlouthi, 1996; Kizil et al., 2002)
—	1389.4	C—H symmetric bending of CH <sub>3</sub> (Kacurakova and Mathlouthi, 1996; van Soest et al., 1995)
1333.7	1333.7	COH bending, CH <sub>2</sub> twisting (Kacurakova and Mathlouthi, 1996; Kizil et al., 2002)
—	1307.8, 1271.3	CH <sub>2</sub> OH side chain related and COH deformation mode (Cael, Koenig, & Blackwell, 1975; Kacurakova and Mathlouthi, 1996; Kizil et al., 2002)
1240.6	—	
1202.1	—	Coupling of C—O and C—C stretching and COH contribution (Kizil et al., 2002; van Soest et al., 1995)
1150.3	1161.8	
1135.9	1135.9	
1106	1106	
1079.2	1087.9	C—O—H bending (Cael et al., 1975)
—	1041.7	Characteristic of crystalline region of retrograded starch
1014.9	1024.5	Characteristic of amorphous region of starch
1000.4	975.5	H-bonding of OH group at C6
929.37	—	Skeletal mode of vibrations of $\alpha$ -1,4 glycosidic linkage (Cael, Koenig, & Blackwell, 1973; Cael et al., 1975; Kizil et al., 2002; Sekkal, Dincq, Legrand, & Huvenne, 1995)
859.26	859.26	C(1)—H, CH <sub>2</sub> deformation
765.13	749.77	C—C stretching (Cael et al., 1973, 1975)
705	705	708.2: skeletal modes of C—C stretch (Sekkal et al., 1995)

<sup>a</sup> Corresponding references for the band assignments are given in parentheses ( ).

within crystalline lamellae and/or to better orientation of crystallites to the X-ray beam. The low crystallinity in lentil starch emphasizes the difference in molecular composition (high amylose content) of lentil starch (Table 1) compared to that of two other starches. Sandhu and Lim (2008) have observed a negative correlation between crystallinity and amylose content for legume starches.

### 3.1.5. FTIR band investigation

The infrared spectra of three starches are compared in Fig. 4(a). The characteristic bands of starch in FTIR spectra can be divided into four main regions. These regions are as follows: below  $800\text{ cm}^{-1}$ ,  $800\text{--}1500\text{ cm}^{-1}$  (the fingerprint region),  $2800\text{--}3000\text{ cm}^{-1}$  (C—H stretching regions), and finally between  $3000$  and  $3600\text{ cm}^{-1}$  (O—H stretching region). The hydroxyl groups are the dominant functional groups in carbohydrates and they are involved in intra and inter-molecular hydrogen bonding with other hydroxyl groups (Ottenhof, MacNaughtan, & Farhat, 2003). The major peaks and their band assignments from the literature (Table 2) observed for starches were at  $3330\text{ cm}^{-1}$  (O—H stretching),

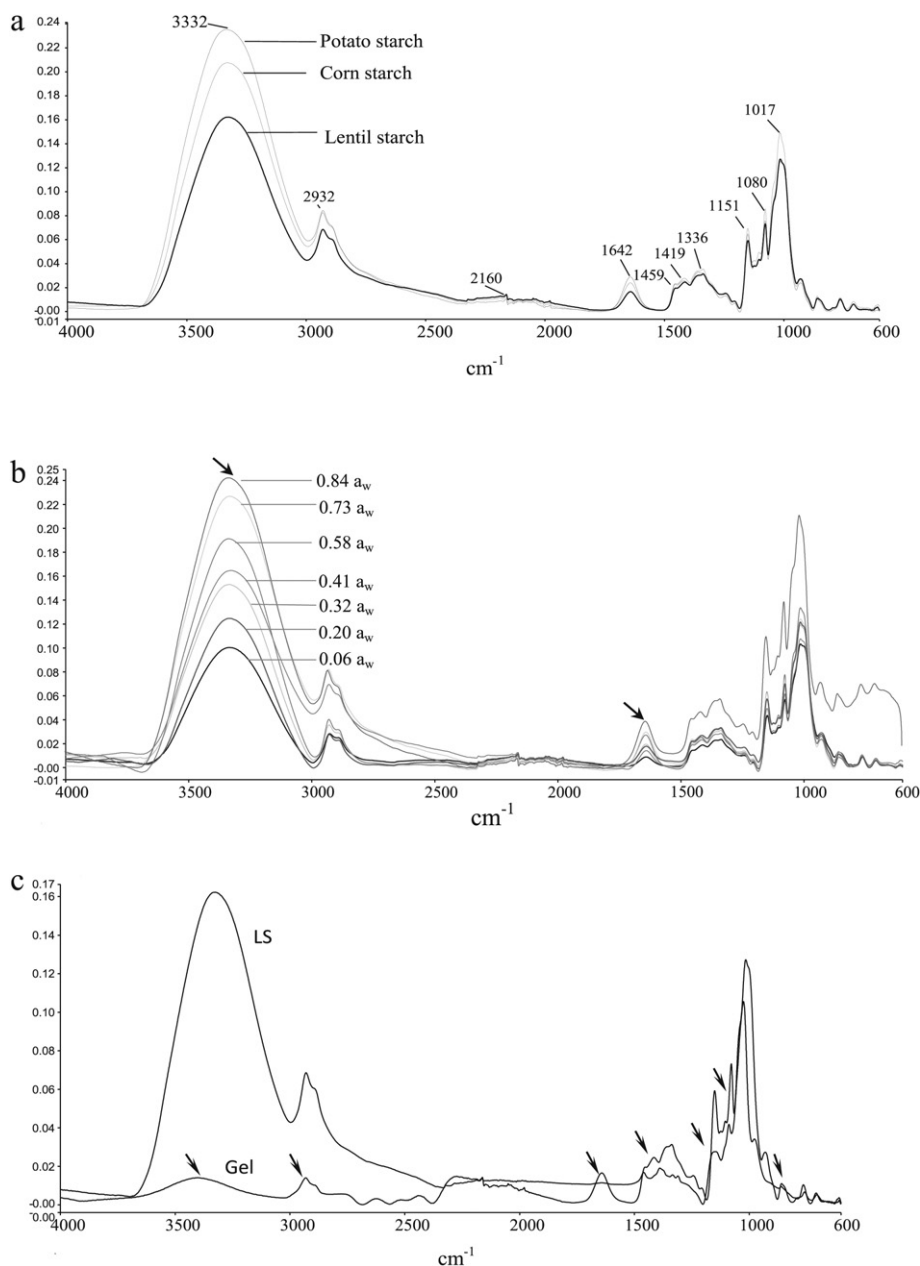


**Fig. 4.** (a) FTIR spectrum of lentil, corn and potato starches in native state showing major peaks ( $\text{cm}^{-1}$ ); (b) effect of hydration: FTIR spectrum of lentil starches at different water activity,  $a_w$  (0.06–0.84) showing effect at major peaks with arrow heads (3332 and  $1642\text{ cm}^{-1}$ ); (c) FTIR spectrum of lentil starch and its gel (12%, w/v) showing major changes in peaks with arrow head.

$2930\text{ cm}^{-1}$  ( $\text{C-H}_2$  stretching),  $1640\text{ cm}^{-1}$  (water bending),  $1450\text{ cm}^{-1}$  ( $\text{CH}$  bending of  $-\text{CH}_2$ ),  $1340\text{ cm}^{-1}$  ( $\text{CH}_2$  twisting),  $1150\text{ cm}^{-1}$  ( $\text{C-O}$  and  $\text{CH}_2$  stretching),  $1014\text{ cm}^{-1}$ ,  $931\text{ cm}^{-1}$  (skeletal mode vibrations of  $\alpha$ -1,4 glycosidic linkage),  $855\text{ cm}^{-1}$  ( $\text{C(1)-H}$ ,  $\text{CH}_2$  deformation) and  $704\text{ cm}^{-1}$  (skeletal mode of  $\text{C-C}$  stretching). The broad band between  $3000$  and  $3600\text{ cm}^{-1}$  was attributed by the vibrational stretches of hydroxyl groups amongst neighbouring molecules of starch (Zhang & Han, 2006). The intensities of some of the major peaks of three starches related to  $\text{O-H}$  stretching and water bending were noticeably different. The order of peak intensity at  $3330\text{ cm}^{-1}$  and  $1640\text{ cm}^{-1}$  was in the following order: potato starch > corn starch > lentil starch.

The IR spectra for lentil starch at different water activity (0.06–0.84) are shown in Fig. 4 (panel b). Though, spectral pattern was similar for all the spectra, the intensity of the peaks related to the water content at  $1642\text{ cm}^{-1}$  decreased as the water

activity decreased from bottom to the top as can be seen in Fig. 4(b). Kizil, Irudayaraj, and Seetharaman (2002) reported that the variation in the crystallinity of starch can affect this band and that as the crystallinity increases the band becomes weaker. Except for the spectra at these two water activities (0.840 and 0.06), IR spectra of all the starches at intermediate water activity values had similar peak intensity at  $1200$ – $1000\text{ cm}^{-1}$  region. The peak at  $1000\text{ cm}^{-1}$  is recognized as water sensitive and is related to intramolecular hydrogen bonding of hydroxyl groups (van Soest, Tournois, de Wit, & Vliegthart, 1995).

Fig. 4(c) compares the IR spectra for lentil starch in native and in gelled (12%, w/v) forms. It can be seen from this figure that some alteration in some of the major peaks and evolution of new peaks occurred due to gel formation (gelatinization). Details of these bands are listed in Table 2 along with the band assignments from the literature for the starch spectra. It is interesting

to note that, the intensity of peak at  $3326\text{ cm}^{-1}$  (related to OH stretching) was greatly decreased and the peak at  $1642\text{ cm}^{-1}$  (water related band) was also disappeared in the gel form compared to the native starch. [Iizuka and Aishima \(1999\)](#) also found similar results for potato and corn starch during heating starches at different temperature. This indicates that water present in the native starch was in free form and, therefore, H–O–H stretch and –OH stretch mode could be detected in IR spectral bands. Whereas after gel formation, the water trapped in starch gel network and does not contribute to absorption of IR energy. The band at  $1416.3\text{ cm}^{-1}$  has shifted to lower wavenumbers  $1389.4\text{ cm}^{-1}$ , while some bands have shifted to higher wavenumbers. For example,  $1079.2\text{ cm}^{-1}$  shifted to  $1087.8\text{ cm}^{-1}$ ;  $1014\text{ cm}^{-1}$  shifted to  $1024.5\text{ cm}^{-1}$ ;  $930\text{ cm}^{-1}$  shifted to  $957.47\text{ cm}^{-1}$  and some new peaks were evolved in the fingerprint region ( $1307\text{ cm}^{-1}$ ,  $1240.6\text{ cm}^{-1}$  and  $1202.1\text{ cm}^{-1}$ ). The spectral region of  $1300\text{--}1200\text{ cm}^{-1}$  is particularly sensitive to the effect arising from hydrogen bonding with other molecule with a high contribution from the asymmetrical deformation ( $\text{CH}_2$  twisting) and from out of ring CH deformations, including bending C–1–H. Intermolecular hydrogen bonding determines the orientation of CH and  $\text{CH}_2$  in  $\text{CH}_2\text{OH}$  whereas most other interactions take place through water molecules ([Kacurakova & Mathlouthi, 1996](#)).

### 3.1.6. Gelatinization properties

Gelatinization is associated with most of the functional properties of starch. The gelatinization parameters of the lentil, corn and potato starches are presented in [Table 1](#). Among the starch samples, corn starch had the highest onset ( $68.58^\circ\text{C}$ ) and peak ( $73.80^\circ\text{C}$ ) gelatinization temperatures while potato starch had the lowest onset ( $60.43^\circ\text{C}$ ) and peak ( $65.65^\circ\text{C}$ ) gelatinization temperatures. The onset and peak gelatinization temperatures for lentil starch were  $61.56^\circ\text{C}$  and  $68.32^\circ\text{C}$ , respectively which are intermediate to those of potato and corn starches. Gelatinization temperatures for lentil, corn and potato starches in this work are close to those reported by [Kaur et al. \(2010\)](#) and [Li and Yeh \(2001\)](#). According to [Tester \(1997\)](#), the gelatinization properties are greatly affected by the molecular structure of amylopectin, amylose/amylopectin ratio and the extent of lipid complexed with amylose chain. Earlier studies have shown that higher transition temperature for corn starch can be attributed to its higher lipid content and more compact granular structure ([Singh, Singh, Kaur, Sodhi, & Gill, 2003](#)). The potato and lentil starches contain only negligible lipid and these starches have larger granules with less compact granular structure ([Hoover & Sosulski, 1991](#)).

Enthalpy of gelatinization was significantly different in these three starches ( $p < 0.05$ ). Among these starches, the lentil starch had the lowest enthalpy of gelatinization ( $11.8\text{ J/g}$ ) while the potato starch had the highest enthalpy ( $18.28 \pm 0.23\text{ J/g}$ ). The degree of crystallinity and enthalpy of gelatinization followed same order ([Table 1](#)). Low enthalpy of gelatinization for lentil starch might be due to its low crystallinity ([Moorthy, 2002](#)). [Li and Yeh \(2001\)](#) also reported higher enthalpy value of  $16.8\text{ J/g}$  for potato starch compared to cereal and legume starches. The variation in gelatinization enthalpy is considered primarily due to energy required for ‘melting’ of crystallites which involves rupture or breakage of intrahelical hydrogen bonds. When starch gelatinizes and swells, double helices formed by amylopectin molecules in crystalline regions uncoil and dissociate as hydrogen bonds are broken. The hydroxyl groups in glucose units become free to hydrogen bond with water. This process has been described as ‘melting’. Earlier, [Cook and Gidley \(1992\)](#), had proposed that enthalpy of gelatinization is principally due to loss of double helical order in starch. However, according to [Lopez-Rubio, Flanagan, Gilbert, and Gidley \(2008\)](#), the enthalpy associated with granule gelatinization is due

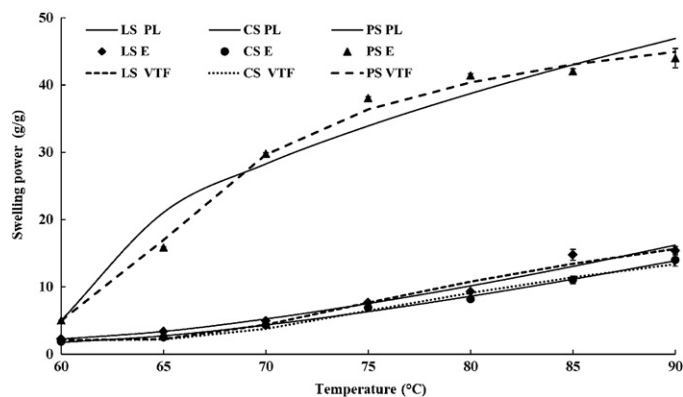


**Fig. 5.** Swelling curve for lentil (LS), corn (CS) and potato starches (PS) showing experimental (E) and VTF (VTF) and power law (PL) model fit data.

to melting of overall amylopectin crystals rather than separation of double helices within starch crystallites. This is also supported by the X-ray diffraction study by [Zobel, Young, and Rocca \(1988\)](#) in which they have reported that gelatinization is the melting of starch crystallites. Since amylopectin mostly exists in crystalline form in starch granules, higher amylopectin content in potato starch requires higher enthalpy for gelatinization. These results indicate that gelatinization enthalpy depends on the magnitude of crystalline fraction which in turn depends on the composition of starch granule (amylose/amylopectin ratio).

When lentil starch suspension was heated to  $60^\circ\text{C}$  (below its gelatinization temperature), no obvious change was observed in normal microscopic view ([Fig. 1](#), panel e) while broadening of Maltese-cross from the centre of the granule was observed ([Fig. 1](#), panel f) in polarized light, indicating loss of birefringence starting from the interior of the granule. [Buléon, Delage, Brisson, and Chanzy \(1990\)](#) also reported similar type of birefringence loss for pea starch having C type of diffraction pattern and attributed it to the heterogeneity in starch granule. They found that the interior of the granule was composed of B polymorph which melted first during gelatinization while A polymorph was located on the periphery. When starch suspension was heated above its peak gelatinization temperature ( $70^\circ\text{C}$ ), no birefringence was observed in polarized light signifying complete melting of all crystallites.

## 3.2. Functional properties of starches

### 3.2.1. Swelling characteristics

Swelling behaviour of lentil starch was investigated over a temperature range of  $60\text{--}90^\circ\text{C}$  and compared to that of corn and potato starches ([Fig. 5](#)). The swelling power was found to increase with increase in the temperature in all these starches. Among three starches, potato starch showed notably higher swelling power at all temperatures beyond  $60^\circ\text{C}$ . In contrast to this, lentil and corn starches exhibited lower swelling power ([Fig. 5](#)). [Vasanthan and Hoover \(1992\)](#) also reported similar trend of swelling for these starches. Cereal and legume starches have limited swelling ability compared to tuber starch ([Leach et al., 1959](#)). The extent of swelling is largely related to their amylose to amylopectin ratio with higher proportions of amylopectin leading to higher swelling. Another possible reason for lower swelling might be higher gelatinization temperature of lentil and corn starch compared to potato starch ([Table 1](#)). According to [Leach et al. \(1959\)](#), higher gelatinization temperature is linked with a higher degree of association in amorphous areas which leads to the restricted swelling in cereal starch. The characteristics of the bonding forces within the starch granules affect the manner with which they undergo swelling. A highly associated starch with an extensive and strongly bonded micellar



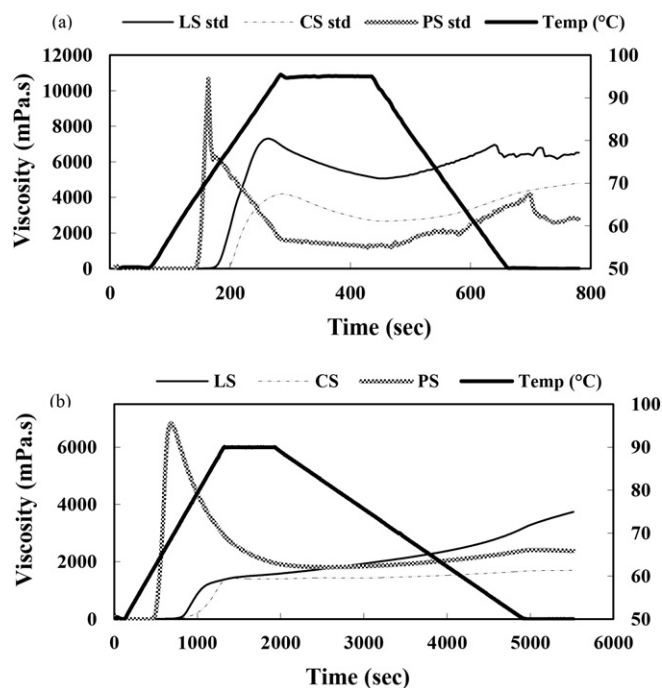


**Fig. 6.** Effect of heating rate on RVA curve (a) at 12.5 °C/min heating and cooling (standard protocol) and (b) slow rate (heating and cooling at 2 °C/min and 0.5 °C/min respectively).

structure is relatively resistant towards swelling and uptake than that of corn and lentil starches. The higher swelling capability of potato starch can also be attributed to its higher content of phosphate groups. It is believed that the repulsion between phosphate groups in adjacent chains helps increase hydration by weakening the bonding within crystalline domain (Galliard & Bowler, 1987).

The swelling power as a function temperature was predicted using VTF and Power law models as shown in Fig. 5. The swelling behaviour of lentil and corn starches was predicted well by both the models ( $R^2 > 0.97$ ). In the case of potato starch, VTF model predicted the swelling data excellently ( $R^2 > 0.99$ ) while power law did not follow the experimental data that well ( $R^2 > 0.95$ ).

### 3.2.2. Pasting characteristics

Pasting is the phenomenon indicated by increase in viscosity when starch is heated in presence of excess of water. Heating causes disruption of internal ordered structure and amylose starts to leach out from the granules. Due to heating and plasticization effect of water, hydrogen bonds stabilizing the crystalline structure in the amylopectin are destabilized and water form hydrogen bonds with amylopectin leading to hydration and swelling. The starch granules become increasingly susceptible to shear disintegration due to swelling. The phase transition in starch was monitored by viscometric method using RVA. The results of pasting properties of lentil starch along with the corn and potato starches are presented in Fig. 6(a) as a plot of apparent viscosity (mPa.s) versus time. The parameters obtained from pasting curve are listed in Table 3. Peak viscosity is related to the granule swelling. Among starches, potato

starch exhibited the highest peak viscosity (10,668 mPa.s) and the lowest pasting temperature of 66.2 °C (temperature at which the viscosity starts to rise). The degree of swelling and granule integrity is directly related to the viscosity of cooked paste. The higher thermal stability of corn and lentil starch can be related to their lower swelling capability. The lower swelling ability and higher gelatinization temperature in lentil and corn starches suggest the presence of strong bonding forces (Hoover & Sosulski, 1991) within these two starch granules as discussed in preceding section.

Lentil starch has shown the intermediate peak value of 7308 mPa.s with peak time of 4.4 min both of which are close to those of corn starch. The observed peak viscosity of lentil starch was about two third value of potato starch and is nearly two fold higher than that of corn starch. Although the pasting behaviours of these three starches are similar to those reported in literature, however, the pasting parameters such as peak and final viscosity are different and cannot be compared due to difference in concentration, method and cultivars used in other published works (Hoover & Manuel, 1995; Li & Yeh, 2001; Sandhu & Lim, 2008). When these starches were heated (with continuous shearing) beyond the point at which peak viscosity was obtained, all the three starches exhibited similar trend of decrease in viscosity. Potato starch with the highest peak viscosity also had higher break-down value compared to lentil and corn starches. This can be attributed to its higher deformability of starch granules due to its very high swelling power (Fig. 5). The break-down value gives an indication of paste stability and is the result of rupture of swollen starch granules. Only intact swollen starch granules contribute to viscosity. When the system is cooled, the amylose leached into the aqueous phase starts to re-associate and gradually forms a gel. The gel formation leads to the final equilibrium viscosity. This increase in viscosity from break down value to final equilibrium viscosity is known as setback in pasting curve. Final viscosity of starch paste when cooled to 50 °C was in following order: lentil starch > corn starch > potato starch. The order of final viscosity of starch gel matches with their amylose content. During the cooling phase, the viscosity of starch paste depends on the nature of starch and the applied shear rate. Cold paste viscosity depends mainly on the composition of the continuous phase which in turn depends on the amount of amylose leached out from the starch granules during heating (Loh, 1992). This is due to tendency of amylose molecules to re-associate strongly upon cooling as the H-bonds between amylose molecules become less transient as the temperature declines. Amylopectin also begins to self-associate but the rate of aggregation or recrystallization is much slower. Therefore, amylose plays an important role in the gel network stabilization in the early stage of gelation. Since the amylose content of lentil starch was significantly higher than other two starches (Table 1), it can be expected that higher concentration of amylose in the continuous phase contributed to the formation of firm gel. These results show that lentil starches can be potentially used where strong gelling properties were required in the final product.

The effect of slow heating (2 °C/min) and cooling (0.5 °C/min) rate on the pasting characteristics of starches was compared with the pasting characteristics under standard protocol (faster heating and cooling at 10 °C/min) (Fig. 6). As can be seen from Fig. 6 (panel b) the breakdown in viscosity in pasting curve was not observed in

**Table 3**  
Pasting properties of lentil, corn and potato starch.

	Peak viscosity (mPa.s)	Peak temperature (°C)	Peak time (min)	Break down (mPa.s)	Set back (mPa.s)	Final viscosity (mPa.s)
Lentil starch	7308	71.9	4.40	2244	1440	6516
Corn starch	4200	76.9	4.80	1536	2112	4776
Potato starch	10,668	66.2	2.73	9492	1608	2772

lentil and corn starches when slow heating and cooling rates were applied. In contrast to this, the pasting curve of potato starch was not affected by heating/cooling rate change due to its low amylose content. The slow cooling rate allowed sufficient time for the formation of gel network with high amylose containing starches like lentil and corn starch while potato starch could not form strong gel network. This means less cohesion amongst granule components resulting into easier disintegration of granules and large fall in viscosity (Fig. 6, panel a). Earlier works (Han & Hamaker, 2001; Jane et al., 1999; Karim et al., 2007) have shown that peak viscosity and the stability of viscosity against shear rate are influenced by amylose content, proportion of amylopectin chain lengths and phosphorus content (Lu, Donner, Yada, & Liu, 2011). These results suggest that pasting characteristics can be manipulated by judiciously using heating and cooling rates for starch granules with weak swelling characteristic such as corn and lentil starch.

### 3.2.3. Gelling characteristics

**3.2.3.1. Dynamic rheological characteristics.** In a dynamic rheological measurement, heat induced gel formation can be followed by monitoring storage modulus,  $G'$  and loss modulus,  $G''$  against time. The effect of heating on the storage modulus ( $G'$ ) of the lentil starch along with the corn and potato starches is shown in Fig. 7 (panel a). As can be seen from figure, sol to gel phase transition of starch suspension induced by heat can be divided into three phases: induction, evolution and equilibrium phases. In the 'induction phase' starch granules continue to swell with the increase in temperature and amylose leaches out from the granules due to weakening of hydrogen bonds holding granules together. No noticeable change in  $G'$  was observed during this phase signifying no gel network formation. In the 'evolution phase'  $G'$  sharply increased many times within short period. This can be explained as follows: starch granules start to disrupt due to limited swelling power and the amylose starts to leach out into the aqueous solution. Amylose is known to form junction zones that support the structure of the incipient and weak gel. At this point, the critical concentration of amylose (in aqueous medium) required to form gel network is attained which results into rapid increase in  $G'$ . The cross-over between  $G'$  and  $G''$  (not shown in Figure) was also observed in this phase. After cross-over point,  $G'$  start to dominate  $G''$  indicating sol to gel phase transformation. The final phase is the 'equilibrium phase' in which  $G'$  quickly attains steady value within few minutes. No change in  $G'$  value was observed in cooling period from 90 °C to 60 °C. The gelation time (defined as the time at which  $G'$  value rises abruptly) for three starches was in following order: potato starch < corn starch < lentil starch. Final elastic modulus ( $G'$ ) at the end of cooling period was the highest for lentil starch ( $11,073 \pm 100$  Pa) while it was the lowest ( $1362 \pm 25$  Pa) for potato starch. The corn starch exhibited intermediate value ( $3828 \pm 58$  Pa) for  $G'$ . Similarly, loss tangent values also showed similar trend and that it was in the following order: lentil starch > corn starch > potato starch (data not shown). The high amylose-to-amylopectin ratio also corresponded to higher  $G'$  and lower loss tangent values suggesting that this ratio is one of the deciding factors of firmness of starch gels.

The mechanical spectra for lentil starch along with the corn and potato starch gels at 60 °C and 10 °C are presented in Fig. 7 (panel b). These graphs show that starch gels behaved as viscoelastic solids characterized by the predominance of elastic modulus,  $G'$  over the viscous modulus  $G''$ . Clark and Ross-Murphy (1987) have classified gels on the basis of mechanical spectrum into entanglement networks, covalently cross-linked molecules and physical gels. A covalent gel is frequency independent (slope  $n = 0$ ), while a physical gel shows slight dependence on frequency ( $n > 0$ ). The elastic modulus ( $G'$ ) at 60 °C is almost independent of frequency for all three starch gels evidenced by a slope ( $n$ ) of logarithmic plots of  $G'$  versus

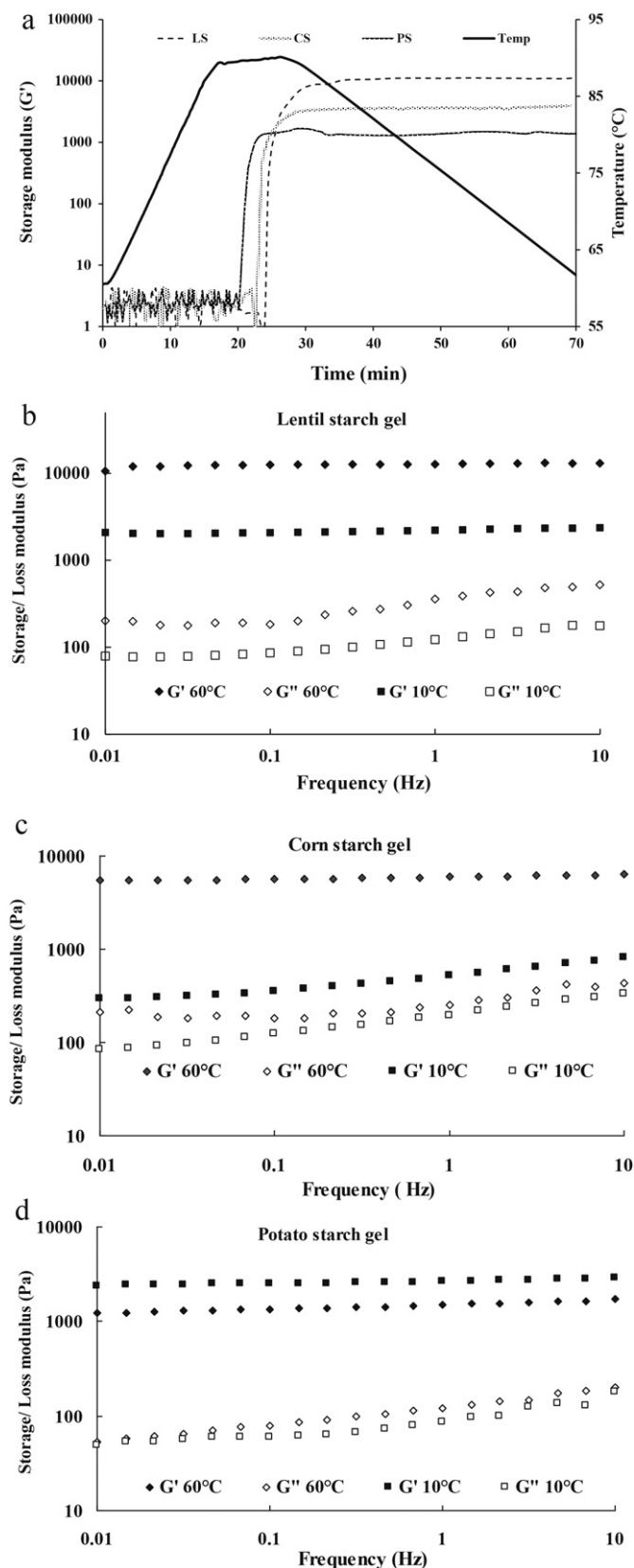


**Fig. 7.** (a) Effect of heating on storage modulus ( $G'$ ) during gel formation for lentil starch (LS), corn starch (CS) and potato starch (PS). (b) Effect of temperature (60 °C and 10 °C) on the mechanical spectra of lentil, corn and potato starch gels.

**Table 4**

Constant ' $n$ ' (slope) value for frequency sweep curve for starch gels (15%, w/v) at 60 °C and 10 °C.

Parameters	Lentil starch	Corn starch	Potato starch
$n$ (60 °C)	0.011	0.029	0.056
$n$ (10 °C)	0.029	0.202	0.037

frequency. Among these three starch gels at 60 °C, the lentil starch gel had the lowest  $n$  value (0.011) closely followed by corn starch gel (0.029) (Table 4). The highest  $n$  value of 0.056 was observed in the case of potato starch gel. However, behaviour of mechanical spectrum at lower temperature (10 °C) was different for all the three starch gels. For lentil and corn starch gel (Fig. 7, panel a and b), the storage modulus showed higher dependence on frequency (Table 4) at 10 °C compared to its frequency dependence at 60 °C suggesting the existence of relaxation process. The magnitude of  $G'$  as well as the difference between moduli ( $G'$  and  $G''$ ) was considerably lower at 10 °C than those at 60 °C indicating a lower percentage of the stored energy recovery. Compared to lentil starch gel, corn starch gel showed greater frequency dependence at lower temperature as can be seen from tenfold increase in  $n$  value at 10 °C compared to its value at 60 °C (Table 4). In contrast to this, the opposite effect was observed in potato starch which showed lower frequency dependence and higher magnitude of storage modulus at 10 °C. The magnitude of  $G'$  and  $G''$  at 10 °C was further apart from each other compared to their values at 60 °C. This might be due to hydrogen bonding in potato starch which is favoured at low temperatures whilst hydrophobic interaction is favoured at high temperatures. The weak variation of  $G'$  with frequency (low slope ( $n$ ) value) and higher magnitude of  $G'$  in lentil and corn starch gels at 60 °C compared to at 10 °C suggest that hydrophobic interaction might be the major stabilizing interaction prevailing in lentil and corn starch gel. Hence, potato starch having low amylose/amylopectin ratio forms better gel structure at low temperatures. Zhang, Gu, Hong, Li, and Cheng (2011) have reported similar results for corn and potato starch gels at 25 °C. Ahmed and Ramaswami (2006) also found that both the moduli ( $G'$  and  $G''$ ) decreased with the increase in temperature in sweet potato puree. Depending on the type of interaction prevailing in the gel formation, these interactions become either stronger (e.g. hydrophobic interactions) or weaker (e.g. hydrogen bonds) with increasing temperature. These results imply that three starch gels behaved differently at different temperatures. The viscous modulus,  $G''$  for all starch gels was found to be more dependent on frequency than elastic modulus,  $G'$  at both temperatures. This type of behaviour is associated with weak gel formation (Clark & Ross-Murphy, 1987; Rosalina & Bhattacharya, 2002).

**3.2.3.2. Texture profile analysis (TPA).** Texture profile analysis (TPA) profiles for lentil starch along with the corn and potato starch gel samples are presented in Fig. 8 (panel a). All the starch gels were significantly different in gel hardness and gumminess properties ( $p < 0.5$ ). Among these three starch gels, lentil starch gel exhibited the highest gel strength and gumminess. Adhesiveness which is defined as the area under negative section of the TPA curve was absent in all three starches. Resilience, cohesiveness and springiness were not significantly different ( $p > 0.05$ ) for all three starches tested. The TPA result showed that lentil starch can form much stronger gel than potato and corn starch gels.

The effect of concentration of lentil starch on gel strength is shown in Fig. 8 (panel b). As the concentration of starch increased from 10 to 40% (w/v), the strength and gumminess also increased accordingly. At lower starch concentration (10–15%, w/v), not much change in gel strength was observed, however, when concentration of starch was increased to 20% (w/v), there was threefold increase in gel strength and gumminess. This result indicates that

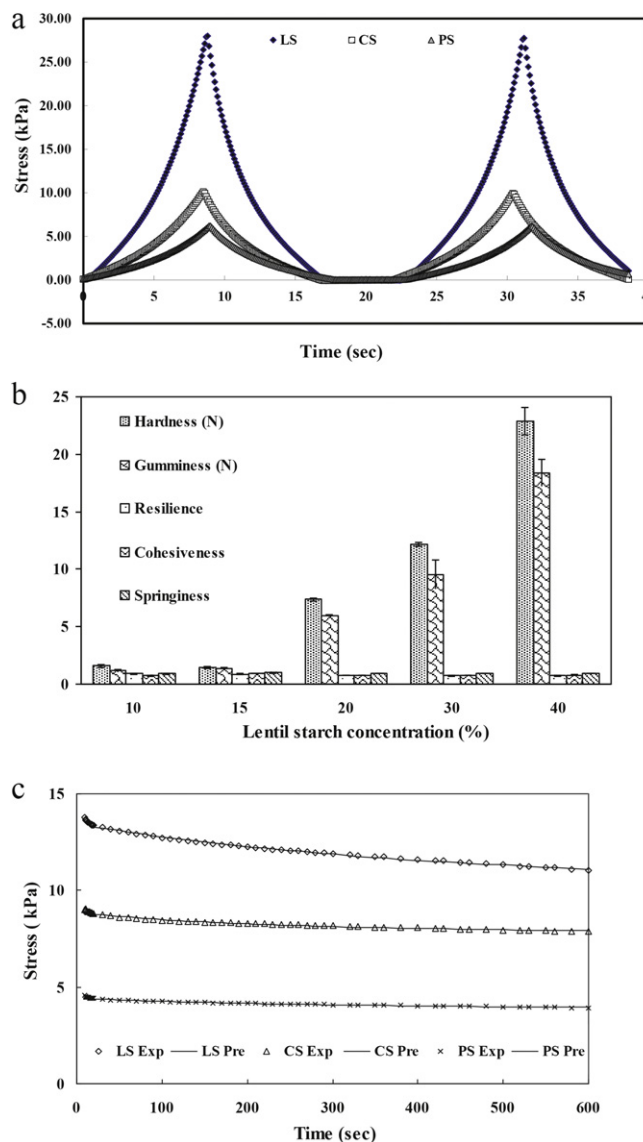


**Fig. 8.** (a) Texture profile analysis (TPA) of starch gels (15%, w/v): lentil starch (LS), corn starch (CS) and potato starch (PS). (b) Effect of lentil starch concentration on texture profile analysis (TPA). (c) Experimental (Exp) and predicted (Pre) stress relaxation curve for lentil, corn and potato starch gels (15%, w/v).

strong interactions among the constituents of lentil starch at higher concentration. Resilience, cohesiveness and springiness value did not change significantly ( $p > 0.05$ ).

**3.2.3.3. Stress relaxation behaviour.** The stress relaxation behaviour of lentils starch along with the corn and potato starch gels was studied and the results are presented in Fig. 8 (panel c). Peleg's model (1980) was used to predict the experimental data and to obtain the rheological parameters (Table 5). Figure shows the typical experimental stress relaxation curves for all the three starches along with their corresponding predicted values (shown by lines) are plotted against the relaxation time. It can be seen that Peleg's model was able to fit experimental data reasonably well with an average absolute error value  $< 0.6\%$  ( $R^2 > 0.97$ ). The graph shows a small gradual decrease in stress over time tending to attain equilibrium stress. This type of behaviour is typical of viscoelastic solid materials. Stress in viscoelastic solids will decay to an equilibrium stress depending on the molecular structure of the material (Figura & Teixeira, 2007). Mean values of model parameters such



**Table 5**

Stress relaxation model parameters starch gels (15%, w/v).

Parameters	Initial stress $\sigma_0$ (kPa)	Equilibrium stress $\sigma_\infty$ (kPa)	$k_1$	$k_2$
Lentil starch	11.82 $\pm$ 1.53	7.85 $\pm$ 0.94	1611 $\pm$ 127	3.02 $\pm$ 0.38
Corn starch	8.16 $\pm$ 0.34	6.94 $\pm$ 0.55	1482 $\pm$ 126	5.90 $\pm$ 0.68
Potato starch	4.89 $\pm$ 0.79	4.02 $\pm$ 0.68	2335 $\pm$ 49	5.60 $\pm$ 0.22

All the data are expressed as mean  $\pm$  SD and are the mean of three replicates.

as initial stress ( $\sigma_0$ ), residual equilibrium stress ( $\sigma_\infty$ ) and the constants  $k_1$  and  $k_2$  are listed in Table 5. The lentil starch gel showed the highest initial (11.82  $\pm$  1.53 kPa) and equilibrium (7.85  $\pm$  0.94 kPa) stress values (Table 5). These initial and equilibrium stress values follow the trend in hardness observed in these three starches in TPA data. The magnitude of constants  $k_1$  and  $k_2$  indicate a more elastic, solid like property in these starch gels. The constant  $k_2$  was not significantly different for corn and potato starch gels. The value of constant  $k_1$  for potato starch gel was significantly higher than those of lentil and corn starch gels ( $p < 0.05$ ). The stress relaxation behaviour of these gels can be attributed to the destruction of weak bonds while the strong bonds remain unaffected by a mechanical deformation of the gels (Hibberd & Wallace, 1966).

#### 4. Conclusions

In this work, the physicochemical (composition, crystallinity, gelatinization behaviour) properties of lentil starch were linked to its functional (swelling, pasting and gel formation) properties and compared with corn and potato starches. The amylose content of these three starches was in the following order: lentil starch > corn starch > potato starch. While crystallinity and enthalpy of gelatinization was in the following order: potato starch > corn starch > lentil. The highest amylose/amylopectin ratio in lentil starch was related to the lowest degree of crystallinity and lowest enthalpy of gelatinization amongst these three starches. The gelatinization and pasting temperature of lentil starch was intermediate between corn and potato starches. Lentil starch gel showed the higher viscoelastic solid properties and gel strength and final viscosity among these three starches. The elastic modulus of lentil starch was eight times higher than that of potato starch and about three times higher than that of corn starch. Peleg's model was able to follow the stress relaxation data of these starch gels well with an average absolute error <0.6% ( $R^2 > 0.98$ ). The elastic modulus of lentil and corn starch gels was less frequency dependent at 60 °C than at 10 °C while the elastic modulus of potato starch was more frequency dependent at 60 °C than at 10 °C. These results suggest that lentil starch can be used in product formulation where stronger gelling properties than that of cereal and tuber starches are required.

#### Acknowledgements

The authors gratefully acknowledge Bruce Armstrong for technical help. The first author gratefully acknowledges the Australian Leadership Award provided by AusAID which enabled this work to be carried out. This work was also partially supported by Australian Government's Collaborative Research Network (CRN) initiative.

#### References

- Adhikari, B., Howes, T., Shrestha, A. K., Tsai, W., & Bhandari, B. R. (2006). Thin-layer isothermal drying of fructose, maltodextrin and their mixture solutions. *Drying Technology*, 24(11), 1415–1424.
- Adsule, R. N., & Kadam, S. S. (1989). Proteins. In D. K. Salunkhe, & S. S. Kadam (Eds.), *Handbook of world food legumes: Nutritional chemistry, processing technology, and utilization* (pp. 75–97). Florida: CRC Press.
- Ahmed, J., & Auras, R. (2011). Effect of acid hydrolysis on rheological and thermal characteristics of lentil starch slurry. *LWT – Food Science and Technology*, 44, 976–983.
- Ahmed, J., & Ramaswami, H. S. (2006). Viscoelastic properties of sweet potato puree infant food. *Journal of Food Engineering*, 74, 376–382.
- Ambigaipalan, P., Hoover, H., Donner, E., Liu, Q., Jaiswal, S., Chibbar, R., et al. (2011). Structure of faba bean, black bean and pinto bean at different levels of granule organization and their physicochemical properties. *Food Research International*, 44(9), 2962–2974.
- AOAC. (2005). *Official methods of analysis* (18th ed.). Arlington, VA: Association of Official Analytical Chemists.
- Bhatty, B. S., & Slinkard, A. E. (1979). Composition, starch properties and protein quality of lentils. *Journal of Institute of Science and Technology Alimentarius*, 12(2), 88–92.
- Biliaderis, C. G., Grant, D. R., & Vose, J. R. (1979). Molecular weight distribution of legume starches by gel chromatography. *Cereal Chemistry*, 56(5), 475–480.
- Bogacheva, T. Y., Wang, Y. L., Wang, T. L., & Hedley, C. L. (2002). Structural studies of starches with different water contents. *Biopolymers*, 64, 268–281.
- Bourne, M. C. (2002). *Food texture and viscosity* (2nd ed.). New York: Academic Press.
- Bul  on, A., Delage, M. M., Brisson, J., & Chanzy, H. (1990). Single crystals of V amylose complexed with isopropanol and acetone. *International Journal Biological Macromolecules*, 12, 25–33.
- Cael, J. J., Koenig, J. L., & Blackwell, J. (1973). Infrared and Raman spectroscopy of carbohydrates. Part III: Raman spectra of the polymorphic forms of amylose. *Carbohydrate Research*, 29, 123–134.
- Cael, J. J., Koenig, J. L., & Blackwell, J. (1975). Infrared and Raman spectroscopy of carbohydrates. Part VI: Normal coordinate analysis of V-amylose. *Biopolymers*, 14, 1885–1903.
- Cheetham, W. H. N., & Tao, L. (1998). Variation in crystalline type with amylose content in maize starch granules: An X-ray powder diffraction study. *Carbohydrate Polymers*, 36, 277–284.
- Chung, H., Liu, Q., & Hoover, R. (2009). Effect of single and dual hydrothermal treatments on the crystalline structure, thermal properties, and nutritional fractions of pea, lentil, and navy bean starches. *Food Research International*, 43, 501–508.
- Clark, A. H., & Ross-Murphy, S. B. (1987). Structural and mechanical properties of biopolymer gels. *Advanced Polymer Science*, 83, 57–192.
- Cook, D., & Gidley, M. J. (1992). Loss of crystallinity and molecular order during starch gelatinization: Origin of the enthalpic transition. *Carbohydrate Research*, 227, 103–112.
- Donovan, J. W. (1979). Phase transitions of starch water systems. *Biopolymers*, 18(2), 263–275.
- Egelandsdal, B., Fretheim, K., & Samejima, K. (1986). Dynamic rheological measurements on heat-induced myosin gels: Effect of ionic strength, protein concentration and addition of adenosine triphosphate or pyrophosphate. *Journal of the Science of Food and Agriculture*, 37(9), 915–926.
- FAO – Food and Agriculture Organization of United Nations. (2010). FAOSTAT Statistics database-agriculture. Rome, Italy.
- Figura, L. O., & Teixeira, A. A. (2007). Food physics. In *Physical properties-measurements and applications: Rheological properties*. New York: Springer.
- Fu, Z. Q., Wang, L. J., Li, D., Wei, Q., & Adhikari, B. (2011). Effects of high-pressure homogenization on the properties of starch-plasticizer dispersions and their films. *Carbohydrate Polymers*, 86(1), 202–207.
- Galliard, T., & Bowler, P. (1987). Morphology and composition of starch. In T. Galliard (Ed.), *Starch properties and potential* (pp. 55–78). Chichester, UK: Wiley.
- Han, X. Z., & Hamaker, B. R. (2001). Amylopectin fine structure and rice starch paste breakdown. *Journal of Cereal Science*, 45, 279–284.
- Hibberd, G. E., & Wallace, W. J. (1966). Dynamic viscoelastic behaviour of wheat Flour Doughs. *Rheologica Acta*, 5(3), 193–198.
- Hoover, H., Hughes, T., Chung, H. J., & Liu, Q. (2010). Composition, molecular structure, properties, and modification of pulse starches: A review. *Food Research International*, 43, 399–413.
- Hoover, R., & Manuel, H. (1995). A comparative study of the physicochemical properties of starches from two lentil cultivars. *Food Chemistry*, 53, 275–284.
- Hoover, R., & Ratnayake, W. S. (2002). Starch characteristics of black bean, chickpea, lentil, navy bean and pinto bean cultivars grown in Canada. *Food Chemistry*, 78, 489–498.
- Hoover, R., & Sosulski, F. (1986). Effect of cross-linking on functional properties of legume starches. *Starch/Starke*, 38(5), 149–155.
- Hoover, R., & Sosulski, F. W. (1991). Composition, structure, functionality, and chemical modification of legume starches: A review. *Canadian Journal of Physiology and Pharmacology*, 69, 79–92.
- Iizuka, K., & Aishima, T. (1999). Starch gelation process observed by FT-IR/ATR spectrometry with multivariate data analysis. *Journal of Food Science*, 64(4), 653–658.



- Jane, J. (1997). Starch functionality in food processing. In P. J. Frazier, P. Richmond, & A. M. Donald (Eds.), *Starch structure and functionality* (pp. 26–35). Cambridge, UK: Royal Society of Chemistry.
- Jane, J., Chen, Y. Y., Lee, L. F., McPherson, A. E., Wong, K. S., Radosavljevic, M., et al. (1999). Effects of amylopectin branch chain length and amylose content on the gelatinization and pasting properties of starch. *Cereal Chemistry*, 76(5), 629–637.
- Jaya, S., & Durance, T. D. (2008). Stress relaxation behaviour of microwave vacuum dried alginate gels. *Journal of Texture Studies*, 39, 183–197.
- Jood, S., Bishnoi, S., & Sharma, A. (1998). Chemical analysis and physico-chemical properties of chickpea and lentil cultivars. *Nahrung*, 42(2), 71–74.
- Kacurakova, M., & Mathlouthi, M. (1996). FTIR and laser-Raman Spectra of oligosaccharides in water: Characterization of the glycosidic bond. *Carbohydrate Research*, 284, 145–157.
- Karim, A. A., Toon, L. C., Lee, V. P. L., Ong, W. Y., Fazilah, A., & Noda, T. (2007). Effects of phosphorus contents on the gelatinization and retrogradation of potato starch. *Journal of Food Science*, 72(2), 132–138.
- Kaur, M., Sandhu, K. S., & Lim, S. (2010). Microstructure, physicochemical properties and in vitro digestibility of starches in different Indian lentil (*Lens culinaris*) cultivars. *Carbohydrate Polymers*, 79, 349–355.
- Kizil, R., Irudayaraj, J., & Seetharaman, K. (2002). Characterization of irradiated starches by using FT-Raman and FTIR spectroscopy. *Journal of Agricultural and Food Chemistry*, 50, 3912–3918.
- Leach, H. W., McCowen, L. D., & Schoch, T. J. (1959). Structure of the starch granule. I. Swelling and solubility patterns of various starches. *Cereal Chemistry*, 36, 534–544.
- Li, J. Y., & Yeh, A. I. (2001). Relationship between thermal, rheological characteristics and swelling power for various starches. *Journal of Food Engineering*, 50, 141–148.
- Lillford, P. J., & Morrison, A. (1997). Structure/function relationship of starches in food. In P. J. In, P. Frazier, A. M. Richmond, & Donald (Eds.), *Starch structure and functionality* (pp. 1–25). Cambridge, UK: Royal Society of Chemistry.
- Loh, J. (1992). The effect of shear rate and strain on the pasting behaviour of food starches. *Journal of Food Engineering*, 16, 75–89.
- Lopez-Rubio, A., Flanagan, B. M., Gilbert, E. P., & Gidley, M. J. (2008). A novel approach for calculating starch crystallinity and its correlation with double helix content: A combined XRD and NMR study. *Biopolymers*, 89(9), 761–768.
- Lu, Z.-H., Donner, E., Yada, R. Y., & Liu, Q. (2011). The synergistic effects of amylose and phosphorus on rheological, thermal and nutritional properties of potato starch and gel. *Food Chemistry*, 133, 1214–1221.
- Moorthy, S. N. (2002). Physicochemical and functional properties of tropical tuber starches: A review. *Starch/Starke*, 54(12), 559–592.
- Nara, S., & Komiya, T. (1983). Studies on the relationship between water saturated state and crystallinity by the diffraction method for moistened potato starch. *Starch/Starke*, 35(12), 407–410.
- Ottenhof, M.-M., MacNaughtan, W., & Farhat, I. A. (2003). FTIR study of state and phase transitions of low moisture sucrose. *Carbohydrate Research*, 338(21), 2195–2202.
- Parker, R., & Ring, S. G. (2001). Aspects of the physical chemistry of starch. *Journal of Cereal Science*, 34(1), 1–17.
- Peleg, M. (1980). Linearization of relaxation and creep curves of solid biological materials. *Journal of Rheology*, 24(4), 451–463.
- Rosalina, I., & Bhattacharya, M. (2002). Dynamic rheological measurements and analysis of starch gels. *Carbohydrate Polymers*, 48, 191–202.
- Sandhu, K. S., & Lim, S. (2008). Digestibility of legume starches as influenced by their physical and structural properties. *Carbohydrate Polymer*, 71, 245–252.
- Sekkal, M., Dincq, V., Legrand, P., & Huvenne, J. P. (1995). Investigation of the glycosidic linkages in several oligosaccharides using FT-IR and FT-Raman spectroscopies. *Journal of Molecular Structure*, 349, 349–352.
- Silverio, J., Fredriksson, H., Andersson, R., Eliasson, A.-C., & Aman, P. (2000). The effect of temperature cycling on the amylopectin retrogradation of starches with different amylopectin unit chain length distribution. *Carbohydrate Polymers*, 42, 175–184.
- Singh, N., Singh, J., Kaur, L., Sodhi, N. S., & Gill, B. S. (2003). Morphological thermal and rheological properties of starches from different botanical sources. *Food Chemistry*, 79, 183–192.
- Tester, R. F. (1997). Starch: The polysaccharide fractions. In P. J. Frazier, P. Richmond, & A. M. Donald (Eds.), *Starch structure and functionality* (pp. 163–171). Cambridge, UK: Royal Society of Chemistry.
- Tester, R. F., Karkalas, J., & Qi, X. (2004). Starch-composition, fine structure and architecture. *Journal of Cereal Science*, 39, 151–165.
- van Soest, J. J. G., Tournois, H., de Wit, D., & Vliegthart, J. F. G. (1995). Short range structure in (partially) crystalline potato starch determined with attenuated total reflectance Fourier-transform IR spectroscopy. *Carbohydrate Research*, 279, 201–214.
- Vasanthan, T., & Hoover, R. (1992). Effect of defatting on starch structure and physicochemical properties. *Food Chemistry*, 45, 337–347.
- Wilson, R. H., Goodfellow, B. J., Beltron, P. S., Osborne, B. G., Oliver, G., & Russell, P. L. (1991). Comparison of Fourier transform mid infrared-spectroscopy and near infrared reflectance spectroscopy with differential scanning calorimetry for the study of the staling of bread. *Journal of Science of Food Agriculture*, 54, 471–483.
- Yao, Y., Zhang, J., & Ding, X. (2002). Structure-retrogradation relationship of rice starches in purified starches and cooked rice grains: A statistical investigation. *Journal of Agricultural and Food Chemistry*, 50, 7420–7425.
- Zhang, Y., & Han, J. H. (2006). Plasticization of pea starch films with monosaccharides and polyols. *Journal of Food Science*, 37(6), 253–261.
- Zhang, Y., Gu, Z., Hong, Y., Li, Z., & Cheng, L. (2011). Pasting and rheological properties of potato starch and maize starch mixtures. *Starch/Starke*, 63, 11–16.
- Zobel, H. F., Young, S. N., & Rocca, L. A. (1988). Starch gelatinization: An X-ray diffraction study. *Cereal Chemistry*, 65(6), 443–446.